Journal of Zhejiang University-SCIENCE B (Biomedicine & Biotechnology)
ISSN 1673-1581 (Print); ISSN 1862-1783 (Online)
www.zju.edu.cn/jzus; www.springerlink.com
E-mail: jzus@zju.edu.cn

Protective effects of parecoxib on rat primary astrocytes from oxidative stress induced by hydrogen peroxide*#

Yun-zhi LING[§1], Xiao-hong LI[§1], Li YU[†‡2], Ye ZHANG[†‡3], Qi-sheng LIANG[1], Xiao-di YANG[4], Hong-tao WANG[5]

([1]*Department of Anesthesiology, First Affiliated Hospital of Bengbu Medical College, Bengbu 233004, China*)

([2]*Department of Laboratory Medicine, Bengbu Medical College, Bengbu 233030, China*)

([3]*Department of Anesthesiology, Second Affiliated Hospital of Anhui Medical University, Hefei 230601, China*)

([4]*Department of Parasitology, Bengbu Medical College, Bengbu 233030, China*)

([5]*Department of Immunology, Bengbu Medical College, Bengbu 233030, China*)

[†]E-mail: yuli95@163.com; zhang_ye011@163.com

Received Jan. 16, 2016; Revision accepted Apr. 10, 2016; Crosschecked Aug. 18, 2016

Abstract: Objective: To investigate the protective effects of parecoxib from oxidative stress induced by hydrogen peroxide (H_2O_2) in rat astrocytes in vitro. Methods: All experiments included 4 groups: (1) negative control (NC) group, without any treatment; (2) H_2O_2 treatment group, 100 μmol/L H_2O_2 treatment for 24 h; (3) and (4) parecoxib pretreatment groups, 80 and 160 μmol/L parecoxib treatment for 24 h, respectively, and then treated with 100 μmol/L H_2O_2. Several indices were investigated, and the expressions of Bax, Bcl-2, and brain-derived neurotrophic factor (BDNF) were quantified. Results: Compared to the NC group, exposure to H_2O_2 resulted in significant morphological changes, which could be reversed by pretreatment of parecoxib. In addition, H_2O_2 treatment led to loss of viability (P=0.026) and increased intracellular reactive oxygen species (ROS) levels (P<0.001), and induced apoptosis (P<0.01) in the primary astrocytes relative to the NC group. However, in the parecoxib pretreatment groups, all the above changes reversed significantly (P<0.05) as compared to the H_2O_2 treatment group, and were nearly unchanged when compared to the NC group. Mechanical investigation showed that dysregulated Bax, Bcl-2, and BDNF could be implicated in these changes. Conclusions: Our results indicated that parecoxib provided a protective effect from oxidative stress induced by exposure to H_2O_2.

Key words: Parecoxib, Primary astrocyte, Hydrogen peroxide (H_2O_2), Brain-derived neurotrophic factor (BDNF), Bax, Bcl-2

http://dx.doi.org/10.1631/jzus.B1600017 **CLC number:** R965

1 Introduction

Elderly patients undergoing surgical intervention often suffer from postoperative cognitive dysfunction (POCD), a condition characterized by progressive deterioration of their cognitive function. POCD can markedly delay postoperative recovery and increase social, financial, and medical burdens. In addition, persistent POCD could develop into dementia, and even lead to the mortality of the patients (Arora *et al.*, 2014). POCD can be diagnosed by

‡ Corresponding authors

§ The two authors contributed equally to this work

* Project supported by the Anhui Education Department (No. KJ2015B004by) and the Bengbu Medical College Innovation Grant (No. BYKY1424ZD), China

Electronic supplementary materials: The online version of this article (http://dx.doi.org/10.1631/jzus.B1600017) contains supplementary materials, which are available to authorized users

ORCID: Ye ZHANG, http://orcid.org/0000-0001-6328-8003

comparing pre- and postoperative psychological parameters using psychometric tests. Though POCD has been observed for several decades, the pathogenesis of POCD remains largely unknown.

It has been widely accepted that, apart from the triggering factor of surgery, many factors contribute to the considerable risks associated with POCD, including old age, pre-existing cerebral, cardiac, and vascular diseases, alcohol abuse, low educational level, and intra- and postoperative complications (Rundshagen, 2014). Oxidative stress is described as a disturbed balance between the generation and elimination of reactive oxygen species (ROS) and reactive nitrogen species (RNS) (Yu *et al*., 2015; Pruchniak *et al.*, 2016), in which condition, antioxidant defense system of the cells cannot coordinate with the increasing ROS and therefore cytotoxicity occurs.

Several sources of evidence indicated that astrocyte is closely implicated with the cognitive function, especially in neurodegenerative diseases with cognitive dysfunction, including Alzheimer and POCD (Phillips *et al.*, 2014; Kim *et al.*, 2015; Hernandez *et al.*, 2016). During the early stages of POCD, astrocytes were abnormally activated and proliferated, which then released a variety of inflammatory cytokines, including interleukin-1 (IL-1), IL-6, and tumor necrosis factor (TNF), and the pro-growth factor S100. These cytokines may lead to pathological changes and repeated neural immune response in the brain, accelerating the deposition of neurotoxic β-amyloid peptide (Aβ) and the formation of neurofibrillary tangles. Neuronal damage and loss may finally lead to cognitive dysfunction in patients (Li *et al.*, 2013; Jin *et al.*, 2014). Oxidative stress plays a crucial role in the progress of POCD, in which free radicals attack astrocytes and neurons and sustain the above mentioned pathological changes of the neurons. Supporting the involvement of oxidative stress in POCD, Li *et al.* (2015) performed protein expression profiling analysis of the hippocampus to explore the different proteins between normal control aged rats and aged rats with POCD, and found that oxidative stress-related pathways were dysregulated in POCD. An *et al.* (2013) also reported that oxidative stress, as well as increased iron accumulation, might be involved in the pathogenesis of POCD. However, the underlying molecular pathways associated with oxidative stress in POCD remain largely unknown.

Parecoxib, a nonsteroidal anti-inflammatory drug (NSAID), selectively blocks off the actions of cyclooxygenase 2 (COX-2) enzyme, which was widely used for postoperative pain relief in clinical practice (Lu *et al.*, 2015). Moreover, Salloum *et al.* (2009) showed that parecoxib could inhibit apoptosis in acute myocardial infarction. In this present study, we used the hydrogen peroxide (H_2O_2) exposure method to induce oxidative stress in primary astrocyte and investigated the functions of parecoxib on oxidative stress.

2 Materials and methods

2.1 Primary astrocyte culture

Primary astrocytes were obtained from Sprague Dawley rats (1 to 7 d old). All experiments were approved and supervised by the Institutional Animal Care and Use Committee of the First Affiliated Hospital of Bengbu Medical College (Bengbu, China). All efforts were made to minimize animal suffering and to reduce the number of animals used.

To prepare primary astrocytes, the hippocampus tissue was first aseptically dissected. After removing the meninges, the hippocampus tissue was mechanically scattered in D-Hank's balanced salt solution (Gibco, USA). Then, the hippocampus tissue was digested with 0.05% (0.5 g/L) trypsin at 37 °C for 10 min, followed by digestion termination using a certain volume of Dulbecco's modified Eagle medium/Ham's F-12 medium (DMEM/F12; Gibco, USA). Finally, the cell supernates were filtered through a 200-mesh metal filter at 400*g* for 5 min.

All cells were cultured in DMEM/F12 supplemented by a 10% fetal bovine serum (FBS), 2 mmol/L glutamine, 100 U/ml penicillin, and 100 mg/ml streptomycin under the stable atmosphere of 37 °C, 95% air/5% CO_2 and then saturation in humidity. Oligodendrocytes and microglia were removed by shaking the dishes at 260 r/min overnight and following that with medium exchange. The purity of the primary astrocyte cultures was determined by immunofluorescence using an antibody against glial fibrillary acidic protein (GFAP), an astrocyte-specific marker.

For all experiments, when the primary astrocytes reached confluence on the plate, they were removed

with 0.25% trypsin, diluted with DMEM/F12, and replated into 6-well plates for serial subcultivation. All experiments were carried out when cells nearly reached confluence during the 4th to 7th passages.

2.2 H_2O_2 and parecoxib treatments of primary astrocytes

After the characterization of the astrocyte cultures from newly-born rats, we combined biochemical and morphological tools to explore the responses of the cells to different stimuli. All experiments included 4 groups: (1) negative control (NC) group, without any treatment; (2) H_2O_2 treatment group, primary astrocytes were treated with 100 μmol/L H_2O_2 for 24 h; (3) and (4) parecoxib pretreatment groups, cells were pretreated with 80 and 160 μmol/L parecoxib for 24 h, respectively, and then treated with 100 μmol/L H_2O_2. Parecoxib (Cat. No. 32152, Sigma-Aldrich, USA) was diluted to 10 mmol/L using a serum-free DMEM/F12 medium and then stored at −20 °C for future use. Before each usage, 10 mmol/L parecoxib was diluted to a final concentration of 80 or 160 μmol/L using a serum-free DMEM/F12 medium. During treatment, primary astrocytes were cultured in the normal atmosphere (37 °C, 95% air/5% CO_2, and saturated in humidity).

After these treatments, the primary astrocytes were observed and photographed using an inverted optical microscope (Leica, Germany) and then stained with Wright stain to examine any morphological changes.

2.3 Viability assay

To assess the metabolic activity, methylthiazolyldiphenyl-tetrazolium bromide (MTT) assay (Sigma-Aldrich, USA) was performed in accordance with the manufacturer's instructions. Briefly, primary astrocytes were collected and plated at a density of 5000 cells/well in a 96-well culture dish. Twenty-four hours later, the medium was discarded and the cells were fixed by using methanol. Then, a total of 20 μl of MTT solution at 5 mg/ml was added into each well. After being incubated at 37 °C for 4 h, the MTT solution was replaced by 200 μl of dimethyl sulfoxide (DMSO, Sigma-Aldrich, USA), which was used to dissolve the formazan crystals through dark incubation for 10 min. Absorbance at 570 nm was measured and the growth inhibition rate was calculated with the following formula: inhibition rate=$(1-A_{exp}/A_{con})\times 100\%$, where A_{exp} and A_{con} are the average absorbances of the experimental and control groups, respectively. Three independent experiments were performed for each sample.

2.4 Fluorescence measurement of intracellular reactive oxygen species

Intracellular peroxides were measured by using an oxidation-sensitive fluorescence probe, 2',7'-dichlorodihydrofluorescein diacetate (DCDHF-DA). In brief, the medium was washed twice with phosphate buffered saline (PBS) and the primary astrocytes were incubated, with 10 μmol/L DCDFH-DA for 20 min at 37 °C, in the dark. After removal of the DCDFH-DA, the fluorescence intensities at 488 nm of excitation wave and 525 nm of emission wave were monitored by flow cytometry and the mean fluorescence intensity of 10 000 cells was used to represent the amount of ROS.

2.5 Cell apoptosis assay

Cell apoptosis assays were performed through flow cytometry using propidium iodide (PI) staining (Sigma-Aldrich, USA). The detailed procedures were observed in previous studies (Shen *et al.*, 2015). Briefly, the primary astrocytes were collected, including both floating and attached cells, and then resuspended in 70% pre-cooled ethanol at 4 °C for fixing for more than 24 h. Before flow cytometry, the fixed cells were washed and stained with PI solution (50 μg/ml PI and 25 μg/ml RNase) at 37 °C for 30 min in the dark. Stained cells were measured by fluorescence-activated cell sorting (FACS) using flow cytometry analysis.

2.6 Reverse transcription polymerase chain reaction (RT-PCR)

Total RNA was extracted from the primary astrocytes using a TRIzol reagent (Invitrogen, USA). The purity and concentration of the total RNA were determined at 260 nm/280 nm using spectrophotometry. Complementary DNA was synthesized using a total RNA reverse transcription kit according to the manufacturer's protocol (Tiangen, China). Approximately 1 μg of total RNA was reverse-transcribed in a reaction volume of 20 μl. PCR reaction cycling conditions were performed as follows: 94 °C for 2 min,

followed by 35 cycles of denaturation at 94 °C for 30 s, annealing at 62 °C (*Bcl-2*) or 58 °C (*Bax*) for 30 s, and extension at 72 °C for 30 s, and a single extension at 72 °C for 5 min. The primer sequences were as follows: (1) *Bax*, forward 5'-CCA AGA AGC TGA GCG AGT GTC-3', reverse 5'-TGA GGA CTC CAG CCA CAA AGA-3'; (2) *Bcl-2*, forward 5'-CAA GCC GGG AGA ACA GGG TA-3', reverse 5'-CCC ACC GAA CTC AAA GAA GGC-3'; (3) *β-actin*, forward 5'-TCA TGA AGT GTG ACG TTG ACA TCC GT-3', reverse 5'-CCT AGA AGC ATT TGC GGT GCA CGA TG-3'. Product sizes for *Bax*, *Bcl-2*, and *β-actin* were 377, 450, and 285 bp, respectively. The PCR products were electrophoresed in 1% (0.01 g/ml) agarose gel, stained with ethidium bromide, examined under UV light, scanned, and photographed. The signal intensities were determined by using Tanon imaging software (Tanon, China). Relative amounts of *Bax* and *Bcl-2* mRNA expressions were measured by the signal intensity ratio of *Bax* and *Bcl-2* to *β-actin*, respectively.

2.7 Western blot

Western blot analysis was performed in accordance with previous studies (Jia *et al.*, 2016). The dilution ratios for BDNF and β-actin were 1:1000 and 1:5000, respectively. Densitometric values were normalized using β-actin as an internal control.

2.8 Statistical analysis

All the statistical analyses were performed using GraphPad 5.0 software and Microsoft Excel. The data were expressed as mean±standard error of the mean (SEM), and the two-tailed Student's test was used for comparison of the two groups and a one-way analysis of variance (ANOVA) was applied to compare more than the two groups. $P<0.05$ was considered statistically significant.

3 Results

3.1 Identification of primary astrocytes

The purity of the primary astrocytes was determined by applying the immunofluorescence method using an anti-GFAP primary antibody. As shown in Fig. S1, the GFAP-positive cells (astrocytes) were approximately 95% of all cells. The cell bodies of the astrocytes were large and flat in the polygon or spindle and the cytoplasmic protuberances were bulky and interweaved with each other. In addition, the boundary of the astrocytes was clear.

3.2 Parecoxib resisted morphological changes of the primary astrocytes due to exposure to H_2O_2

Normally, primary astrocytes cultured in vitro showed regular and large cell bodies in the polygon or spindle, and also clear cell boundaries. More importantly, the cells were vibrant (Fig. 1a). However, when they were treated with 100 μmol/L H_2O_2, the cell morphology changed sharply, with shrinking cell bodies and blurry edges (Fig. 1b). We further pretreated the primary astrocytes with parecoxib before H_2O_2 treatment, in order to investigate the protective effect of parecoxib from oxidative stress induced by H_2O_2. From Fig. 1c (80 μmol/L parecoxib) and Fig. 1d (160 μmol/L parecoxib), we found that if the primary astrocytes were pretreated with parecoxib, cell morphology changed mildly after H_2O_2 treatment, suggesting that parecoxib had an obvious protective effect from oxidative stress induced by H_2O_2.

3.3 H_2O_2 exposure led to loss of viability of the primary astrocytes, which was reversed by parecoxib

In order to investigate the effect of H_2O_2 exposure on astrocyte's viability, we treated cells with 100 μmol/L H_2O_2 and applied the MTT method to measure the growth inhibition rate of the astrocytes. Compared to the NC group, the groups treated with H_2O_2 showed a (35.25±0.42)% reduction of viability (P=0.026; Fig. 2). However, if the astrocytes were pretreated with parecoxib, the loss of astrocyte's viability could be reversed by both 80 μmol/L (P=0.038) and 160 μmol/L (P=0.031) parecoxib relative to the H_2O_2 treatment group (Fig. 2).

3.4 Protection of parecoxib from the increase of intracellular ROS levels of primary astrocytes due to exposure to H_2O_2

To investigate whether H_2O_2 exposure influenced the intracellular ROS levels and the potential protective effect of parecoxib from H_2O_2 exposure in primary astrocytes, we treated primary astrocytes with H_2O_2 and parecoxib in different concentrations and measured the intracellular peroxides using DCDHF-DA.

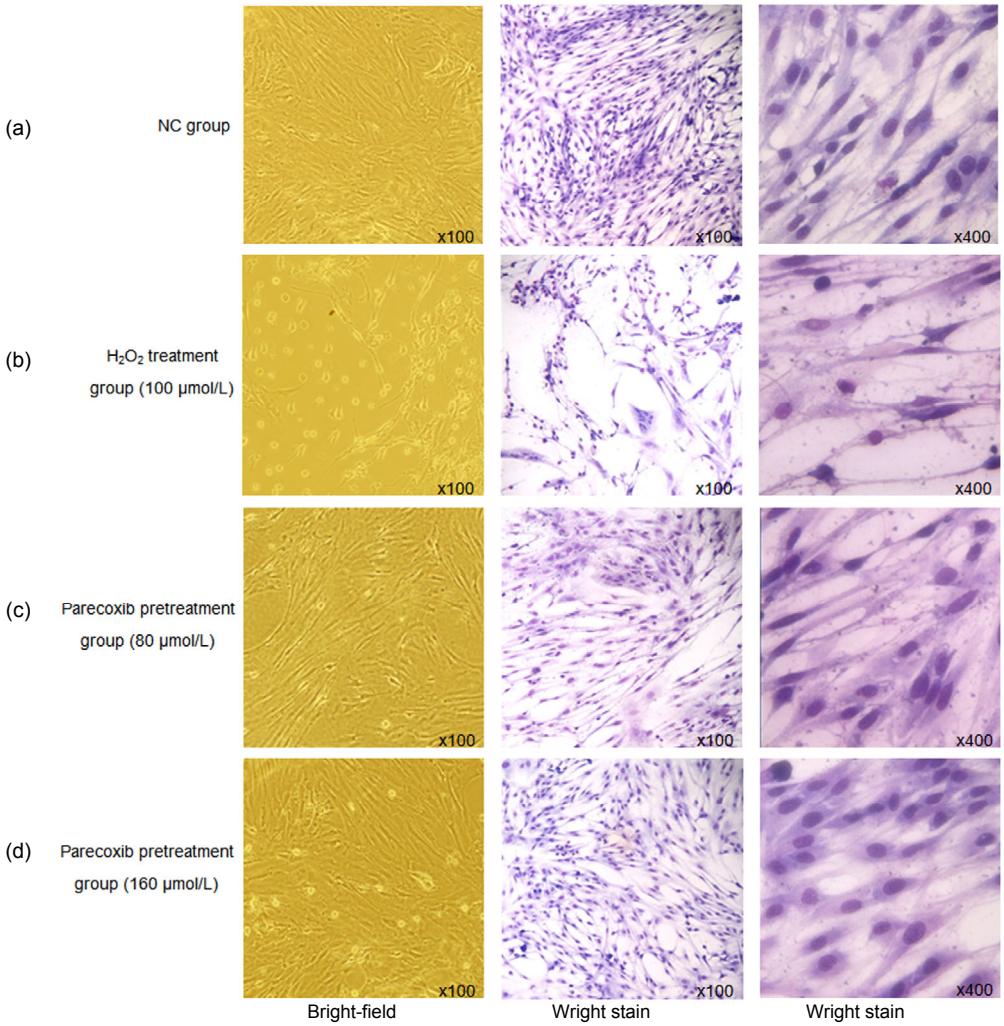

Fig. 1 Parecoxib resisted morphological changes of the primary astrocytes due to exposure to H_2O_2

(a) NC group; (b) H_2O_2 treatment group (100 μmol/L); (c) Parecoxib pretreatment group (80 μmol/L); (d) Parecoxib pretreatment group (160 μmol/L)

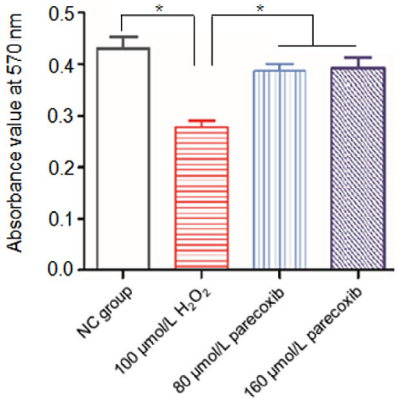

Fig. 2 H_2O_2 exposure led to loss of viability in the primary astrocytes, which was reversed by parecoxib

Data shown were representative of three independent experiments and error bars represent mean±SEM. * P<0.05 vs. H_2O_2 treatment group

When compared to the NC group, the fluorescence intensity of the H_2O_2 treatment group increased significantly (P<0.001), suggesting strengthened ROS levels. However, if the primary astrocytes were pretreated with parecoxib (160 μmol/L) and then exposed to 100 μmol/L H_2O_2, the fluorescence intensity decreased significantly relative to the H_2O_2 treatment group (P<0.01), and more closer to the NC group (P>0.05) (Fig. 3). For the 80 μmol/L pretreatment group, the fluorescence intensity also decreased relative to the H_2O_2 treatment group, but not reaching statistical significance, and significant differences of fluorescence intensity existed between the 80 μmol/L pretreatment group and the NC group as well.

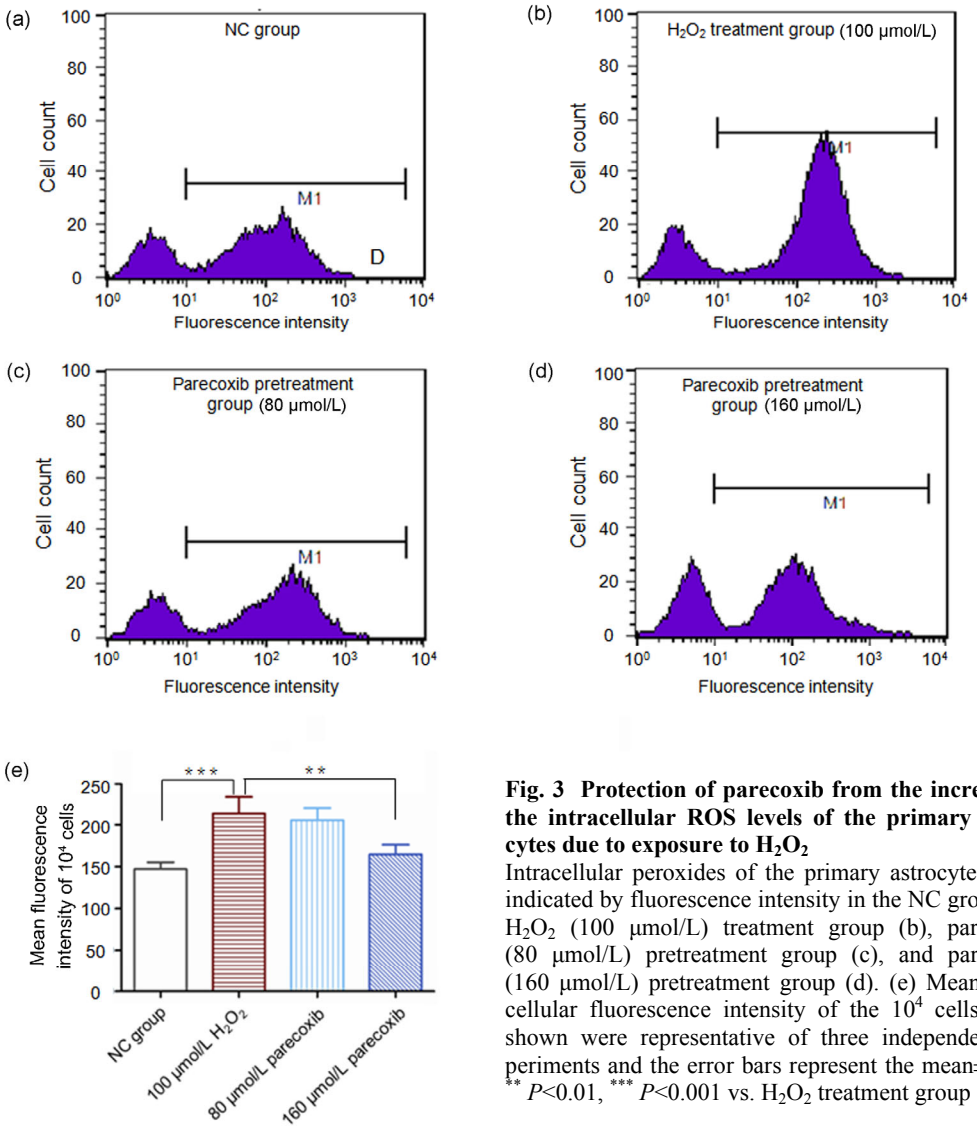

Fig. 3 Protection of parecoxib from the increase of the intracellular ROS levels of the primary astrocytes due to exposure to H_2O_2

Intracellular peroxides of the primary astrocytes were indicated by fluorescence intensity in the NC group (a), H_2O_2 (100 μmol/L) treatment group (b), parecoxib (80 μmol/L) pretreatment group (c), and parecoxib (160 μmol/L) pretreatment group (d). (e) Mean intracellular fluorescence intensity of the 10^4 cells. Data shown were representative of three independent experiments and the error bars represent the mean±SEM. ** P<0.01, *** P<0.001 vs. H_2O_2 treatment group

3.5 Parecoxib resisted apoptosis of the primary astrocytes induced by exposure to H_2O_2

To further explore the apoptosis-induced effect of H_2O_2 on the primary astrocyte and the rescued effect of parecoxib from H_2O_2 exposure, we assessed the extent of cell apoptosis through flow cytometry using PI staining.

The H_2O_2 induced strong cell apoptosis of the primary astrocytes at the concentration of 100 μmol/L, compared to the NC group (34.0% vs. 9.1%, P<0.01). However, if the primary astrocytes were pretreated with parecoxib (80 and 160 μmol/L) and then exposed to 100 μmol/L H_2O_2, the apoptotic rates were 16.5% and 14.6%, respectively, which were significantly decreased relative to the H_2O_2 treatment group (P<0.01) and were comparative with the NC group (P>0.05) (Fig. 4).

3.6 Exposure to H_2O_2 resulted in dysregulated *Bax*, *Bcl-2*, and *BDNF* expressions, which were reversed by parecoxib

In order to explore the possible mechanisms of H_2O_2-induced apoptosis, we performed RT-PCR to quantify the expression levels of *Bax* and *Bcl-2*, both of which were implicated in cell apoptosis in previous studies (Guan *et al.*, 2015; Cao *et al.*, 2016).

Compared to the NC group, the relative expressions of *Bax* and *Bcl-2* in the H_2O_2 treatment group

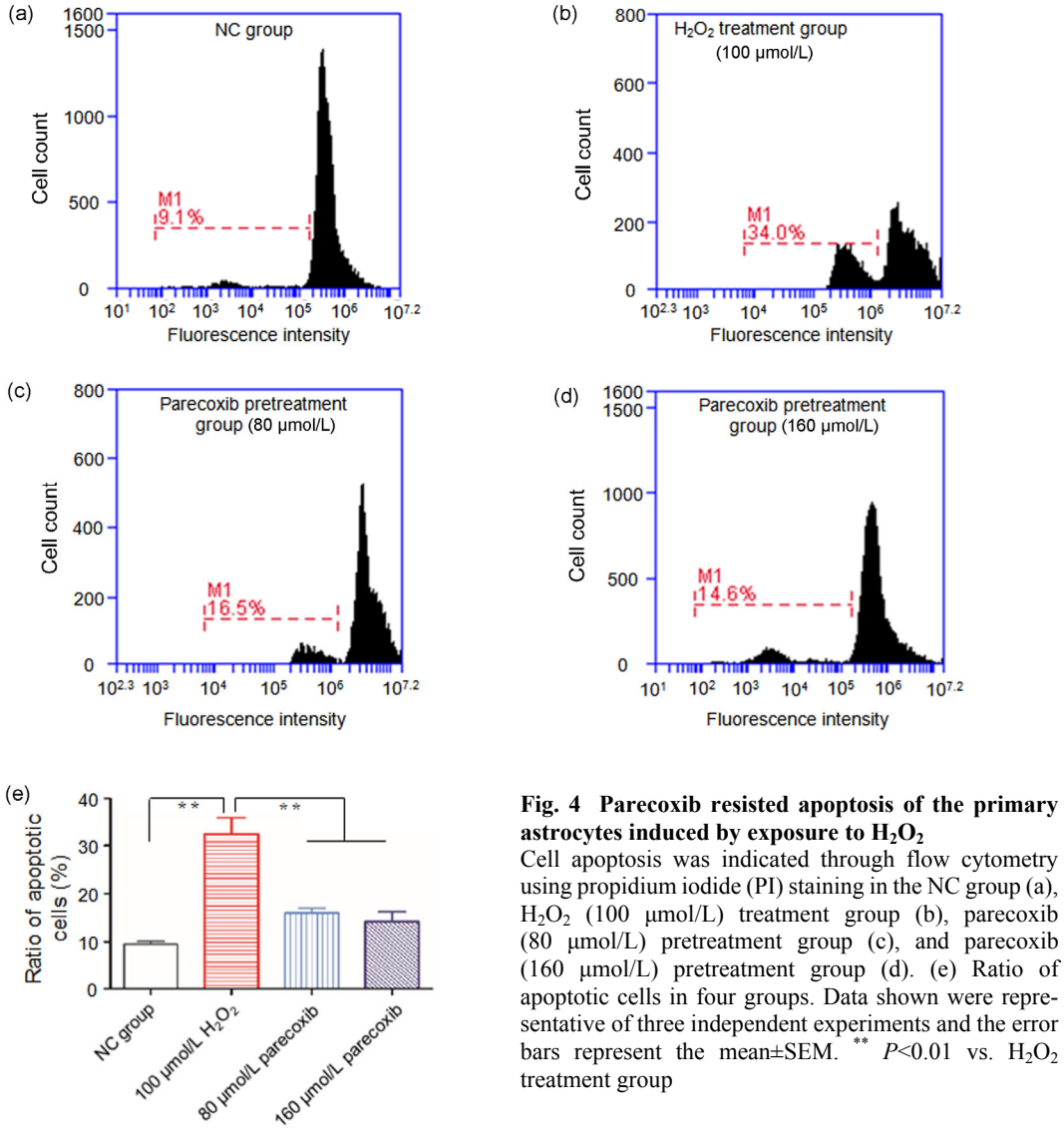

Fig. 4 Parecoxib resisted apoptosis of the primary astrocytes induced by exposure to H_2O_2
Cell apoptosis was indicated through flow cytometry using propidium iodide (PI) staining in the NC group (a), H_2O_2 (100 μmol/L) treatment group (b), parecoxib (80 μmol/L) pretreatment group (c), and parecoxib (160 μmol/L) pretreatment group (d). (e) Ratio of apoptotic cells in four groups. Data shown were representative of three independent experiments and the error bars represent the mean±SEM. ** P<0.01 vs. H_2O_2 treatment group

were significantly increased (P=0.012) and decreased (P=0.038), respectively. In the 160 μmol/L parecoxib pretreatment group, the *Bax* relative expression showed significantly downregulation relative to the H_2O_2 treatment group (P=0.010), and the *Bcl-2* relative expression was statistically upregulated (P=0.037). For the 80 μmol/L parecoxib pretreatment group, the relative *Bax* expression was downregulated and the relative *Bcl-2* was upregulated as well, but not reaching statistical significance, as compared to the H_2O_2 treatment group (Fig. 5).

We also performed the Western blot analysis to quantify the expression levels of *BDNF*. Compared to the NC group, the BDNF expression was significantly decreased (P=0.012). If cells were pretreated by 160 μmol/L parecoxib, the *BDNF* level could be upregulated relative to the H_2O_2 treatment group (P=0.018) (Fig. 6).

4 Discussion

In the present study, we tried to investigate the protective effect of parecoxib from adverse conditions derived from oxidative stress induced by H_2O_2 exposure in primary astrocytes. We observed that H_2O_2 (100 μmol/L) exposure led to loss of viability, morphological changes, increased intracellular ROS

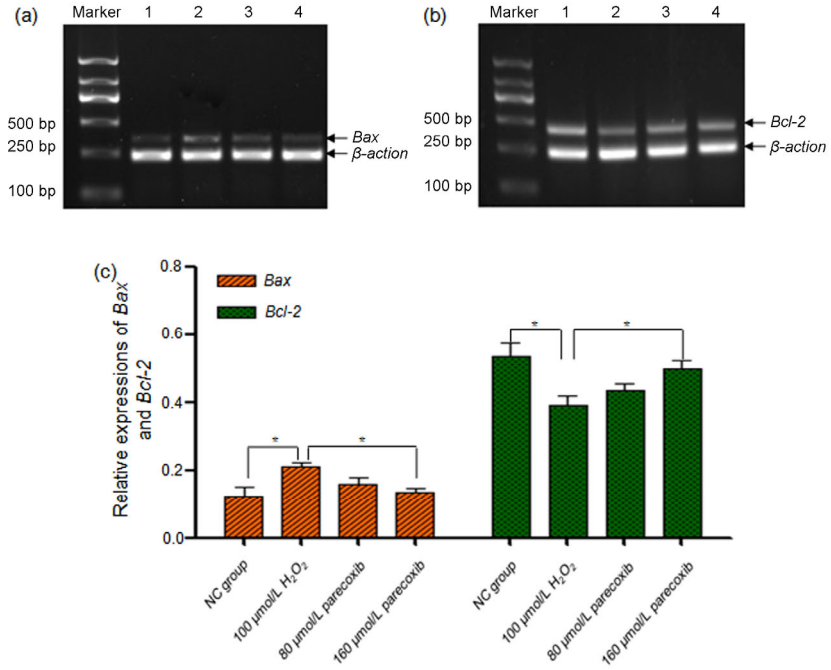

Fig. 5 Exposure to H_2O_2 resulted in dysregulated *Bax* and *Bcl-2* expressions, which were reversed using parecoxib
(a, b) Gel electrophoresis images of the RT-PCR products of *Bax* and *Bcl-2* in four groups: (1) NC group; (2) H_2O_2 (100 μmol/L) treatment group; (3) parecoxib (80 μmol/L) pretreatment group; and (4) parecoxib (160 μmol/L) pretreatment group. *β-Actin* was used as an internal control. The RT-PCR product lengths of *Bax*, *Bcl-2*, and *β-actin* were 377, 450, and 285 bp, respectively. (c) Gray intensity of the gel electrophoresis images of the RT-PCR products of *Bax* and *Bcl-2* in four groups. Data shown were representative of three independent experiments and the error bars represent the mean±SEM. * $P<0.05$ vs. H_2O_2 treatment group

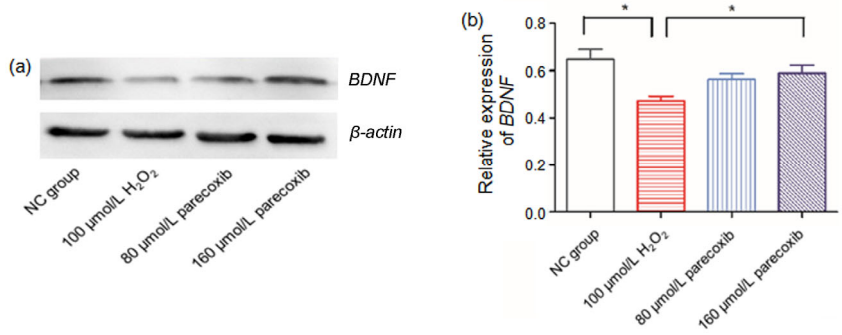

Fig. 6 Exposure to H_2O_2 resulted in dysregulated *BDNF* expression, which was reversed by parecoxib
Data shown were representative of three independent experiments and the error bars represent the mean±SEM. * $P<0.05$ vs. H_2O_2 treatment group. *β-actin* was used an internal control

levels, and apoptosis of the astrocytes cultured in vitro; however, pretreatment of 80 or 160 μmol/L parecoxib could reverse these conditions.

Glial cells account for approximately 90% of the total cells in the nervous system, among which astrocytes are one category representing the largest number. Previous studies showed that astrocytes not only are implicated in formation and maintenance of the blood-brain barrier, and the regulation of synaptic plasticity (Barres, 2008), but also provide energy and metabolic support for neurons (Pellerin *et al.*, 2007).

Oxidative stress is described as the disturbed balance between generation and elimination of the ROS and RNS (Pruchniak *et al.*, 2016), in which condition antioxidant defense system of the cells cannot coordinate with the increasing ROS and therefore cytotoxicity occurs. Several sources of evidence showed that oxidative stress plays an important

role in the development of POCD (An *et al.*, 2013; Li *et al.*, 2015). In the present study, we show that exposure to H_2O_2 increased intracellular ROS levels of primary astrocytes, while pretreatment with parecoxib (160 μmol/L) could reverse the increased intracellular ROS levels.

Mechanical investigation of our study indicated that exposure to H_2O_2 resulted in the increase of *Bax* and decease of *Bcl-2* expression levels, which were reversed by 160 μmol/L parecoxib pretreatment, suggesting that dysregulated *Bax* and *Bcl-2* could mediate oxidative stress induced by H_2O_2 exposure, and the protective effect of parecoxib in the primary astrocytes. Both *Bax* and *Bcl-2* were reported to be implicated in cell apoptosis in previous studies (Guan *et al.*, 2015; Cao *et al.*, 2016). *Bcl-2* is known to be a "survival gene" and its expression level is positively correlated with the cell life span. Zhang *et al.* (2014) have reported that Bcl-2 protein expressed early in the hippocampus in the transient cerebral ischemia animal experiments, exhibited a protective role from cerebral ischemia. *Bax* is a apoptosis promoting gene, which can induce apoptosis through initiating the mitochondrial permeability transition. In addition, Bax may activate cysteine protease and then antagonize the protective effect of Bcl-2 (Smith *et al.*, 2015). Therefore, the expressions of *Bax* and *Bcl-2* could be inversely related, which are consistent with our study.

BDNF is one of the most abundant secretions of astrocytes, and has diverse functions in maintaining survival, development, regeneration, and differentiation of neurons. Valvassori *et al.* (2015) observed that BDNF treatment modulated the antioxidant enzymes, and protected the ouabain (OUA)-induced oxidative damage in the brain of rats. In addition, Takeda *et al.* (2013) showed that BDNF protected human microvascular endothelial cells from the toxicity of TNF-α through the regulation of the PTEN/Akt pathway. All the above evidence suggests that BDNF could play an important role in the protective effect of parecoxib in primary astrocytes. Indeed, we observed significantly downregulated *BDNF* levels of primary astrocytes in the H_2O_2 treatment group when compared to the NC group; however, if cells were pretreated with parecoxib, the expression of *BDNF* was statistically upregulated relative to the H_2O_2 treatment group. Nevertheless, the detailed molecular pathways of BDNF implicated in the protective function of parecoxib still remain to be identified.

One limitation of this study was that we used parecoxib, but not its secondary metabolite by hepatic enzyme in vivo, valdecoxib, for primary astrocyte treatment. Parecoxib is the first injectable COX-2 inhibitor and has been introduced into clinical practice for postoperative pain control since 2001. Compared to valdecoxib, the secondary metabolite by the hepatic enzyme in vivo, parecoxib is prescribed more prevalently in clinical practice. Based on clinical observation, we chose parecoxib, but not valdecoxib, for experimental research. However, since experiments in vitro cannot simulate the in vivo environment, for example, lack of the hepatic enzyme, parecoxib could exert its antalgic function only by itself, but not valdecoxib. This could confer functional divergence of parecoxib between in vitro and in vivo experiments to some extent. It would be essential to conduct in vivo replication of the present studies in the future.

In conclusion, our results indicated that parecoxib (80 and 160 μmol/L) had a protective effect from oxidative stress induced by exposure to H_2O_2. Moreover, dysregulated *Bax*, *Bcl-2*, and *BDNF* could be underpinning the pathological process.

Acknowledgements

We sincerely thank Dr. Shu-quan RAO (School of Life Science and Engineering, Southwest Jiaotong University, Chengdu, China) for providing technical guidance and statistic assistance.

Compliance with ethics guidelines

Yun-zhi LING, Xiao-hong LI, Li YU, Ye ZHANG, Qi-sheng LIANG, Xiao-di YANG, and Hong-tao WANG declare that they have no conflict of interest.

All institutional and national guidelines for the care and use of laboratory animals were followed.

References

An, L.N., Yue, Y., Guo, W.Z., *et al.*, 2013. Surgical trauma induces iron accumulation and oxidative stress in a rodent model of postoperative cognitive dysfunction. *Biol. Trace Elem. Res.*, **151**(2):277-283. http://dx.doi.org/10.1007/s12011-012-9564-9

Arora, S.S., Gooch, J.L., Garcia, P.S., 2014. Postoperative cognitive dysfunction, Alzheimer's disease, and anesthesia. *Int. J. Neurosci*., **124**(4):236-242. http://dx.doi.org/10.3109/00207454.2013.833919

Barres, B.A., 2008. The mystery and magic of glia: a perspective on their roles in health and disease. *Neuron*, **60**(3): 430-440.

http://dx.doi.org/10.1016/j.neuron.2008.10.013

Cao, Y., Jiang, Z., Zeng, Z., *et al.*, 2016. Bcl-2 silencing attenuates hypoxia-induced apoptosis resistance in pulmonary microvascular endothelial cells. *Apoptosis*, **21**(1): 69-84.
http://dx.doi.org/10.1007/s10495-015-1184-3

Guan, J.J., Zhang, X.D., Sun, W., *et al*., 2015. DRAM1 regulates apoptosis through increasing protein levels and lysosomal localization of BAX. *Cell Death Dis.*, **6**:e1624.
http://dx.doi.org/10.1038/cddis.2014.546

Hernandez, R.V., Puro, A.C., Manos, J.C., *et al.*, 2016. Transgenic mice with increased astrocyte expression of IL-6 show altered effects of acute ethanol on synaptic function. *Neuropharmacology*, **103**:27-43.
http://dx.doi.org/10.1016/j.neuropharm.2015.12.015

Jia, S.N., Lin, C., Chen, D.F., *et al.*, 2016. The transcription factor p8 regulates autophagy in response to palmitic acid stress via a mammalian target of rapamycin (mTOR)-independent signaling pathway. *J. Biol. Chem*., **291**(9): 4462-4472.
http://dx.doi.org/10.1074/jbc.M115.675793

Jin, W.J., Feng, S.W., Feng, Z., *et al*., 2014. Minocycline improves postoperative cognitive impairment in aged mice by inhibiting astrocytic activation. *Neuroreport*, **25**(1):1-6.

Kim, G.H., Kim, J.E., Rhie, S.J., *et al*., 2015. The role of oxidative stress in neurodegenerative diseases. *Exp. Neurobiol.*, **24**(4):325-340.
http://dx.doi.org/10.5607/en.2015.24.4.325

Li, R.L., Zhang, Z.Z., Peng, M., *et al.*, 2013. Postoperative impairment of cognitive function in old mice: a possible role for neuroinflammation mediated by HMGB1, S100B, and RAGE. *J. Surg. Res.*, **185**(2):815-824.
http://dx.doi.org/10.1016/j.jss.2013.06.043

Li, Y., Wang, S., Ran, K., *et al*., 2015. Differential hippocampal protein expression between normal aged rats and aged rats with postoperative cognitive dysfunction: a proteomic analysis. *Mol. Med. Rep.*, **12**(2):2953-2960.

Lu, J., Liu, Z., Xia, K., *et al.*, 2015. Effect of preemptive analgesia with parecoxib sodium in patients undergoing radical resection of lung cancer. *Int. J. Clin. Exp. Med*., **8**(8):14115-14118.

Pellerin, L., Bouzier-Sore, A.K., Aubert, A., *et al.*, 2007. Activity-dependent regulation of energy metabolism by astrocytes: an update. *Glia*, **55**(12):1251-1262.
http://dx.doi.org/10.1002/glia.20528

Phillips, E.C., Croft, C.L., Kurbatskaya, K., *et al.*, 2014. Astrocytes and neuroinflammation in Alzheimer's disease. *Biochem. Soc. Trans.*, **42**(5):1321-1325.
http://dx.doi.org/10.1042/BST20140155

Pruchniak, M.P., Arazna, M., Demkow, U., 2016. Biochemistry of oxidative stress. *Adv. Exp. Med. Boil.*, **878**:9-19.
http://dx.doi.org/10.1007/5584_2015_161

Rundshagen, I., 2014. Postoperative cognitive dysfunction. Dtsch. *Arztebl. Int*., **111**(8):119-125.

Salloum, F.N., Hoke, N.N., Seropian, I.M., *et al.*, 2009. Parecoxib inhibits apoptosis in acute myocardial infarction due to permanent coronary ligation but not due to ischemia-reperfusion. *J. Cardiovasc. Pharmacol.*, **53**(6): 495-498.
http://dx.doi.org/10.1097/FJC.0b013e3181a7b5b6

Shen, L., Zhu, J., Chen, F., *et al.*, 2015. RUNX1-Evi-1 fusion gene inhibited differentiation and apoptosis in myelopoiesis: an in vivo study. *BMC Cancer*, **15**(1):970.
http://dx.doi.org/10.1186/s12885-015-1961-y

Smith, C.C., Guevremont, D., Williams, J.M., *et al*., 2015. Apoptotic cell death and temporal expression of apoptotic proteins Bcl-2 and Bax in the hippocampus, following binge ethanol in the neonatal rat model. *Alcohol. Clin. Exp. Res*., **39**(1):36-44.
http://dx.doi.org/10.1111/acer.12606

Takeda, K., Kermani, P., Anastasia, A., *et al*., 2013. BDNF protects human vascular endothelial cells from TNFα-induced apoptosis. *Biochem. Cell Biol.*, **91**(5):341-349.
http://dx.doi.org/10.1139/bcb-2013-0005

Valvassori, S.S., Arent, C.O., Steckert, A.V., *et al.*, 2015. Intracerebral administration of BDNF protects rat brain against oxidative stress induced by ouabain in an animal model of mania. *Mol. Neurobiol.*, **52**(1):353-362.
http://dx.doi.org/10.1007/s12035-014-8873-8

Yu, H.T., Zhen, J., Pang, B., *et al.*, 2015. Ginsenoside Rg1 ameliorates oxidative stress and myocardial apoptosis in streptozotocin-induced diabetic rats. *J. Zhejiang Univ.-Sci. B (Biomed. & Biotechnol.)*, **16**(5):344-354.
http://dx.doi.org/10.1631/jzus.B1400204

Zhang, N., Cheng, G.Y., Liu, X.Z., *et al*., 2014. Expression of Bcl-2 and NF-κB in brain tissue after acute renal ischemia-reperfusion in rats. *Asian Pac. J. Trop. Med.*, **7**(5): 386-389.
http://dx.doi.org/10.1016/S1995-7645(14)60061-4

List of electronic supplementary materials

Fig. S1 Identification of primary astrocytes using GFAP staining

中文概要

题　目：帕瑞昔布对过氧化氢诱导的原代星形胶质细胞氧化应激的保护作用

目　的：评估帕瑞昔布对过氧化氢诱导的大鼠原代星形胶质细胞氧化应激状态的保护作用，并初步探讨其作用机制。

创新点：首次在大鼠原代星形胶质细胞中证实帕瑞昔布对过氧化氢诱导的氧化应激具有保护作用，且此作用可能与 Bax、Bcl-2 和 BDNF 的失调有关。

方　法：设立如下四组对照：(1)阴性对照组；(2)100 μmol/L H_2O_2 处理组（处理时间为 24 h）；(3) 80 μmol/L

帕瑞昔布处理组；（4）160 μmol/L 帕瑞昔布处理组（第三和第四组先用帕瑞昔布处理 24 h，再用 100 μmol/L H_2O_2 处理 24 h）。用荧光显微镜观察星形胶质细胞的形态，用 MTT 法检测星形胶质细胞的存活率，用荧光探针二氯荧光黄双乙酸盐（DCDHF-DA）检测星形胶质细胞内氧自由基的含量，并用碘化丙啶（PI）染色检测细胞的凋亡状态。最后用反转录酶聚合酶链反应（RT-PCR）和蛋白质印迹（Western blot）检测 Bax、Bcl-2 和 BDNF 三种蛋白在 4 组中的表达水平。

结　论：H_2O_2 处理可以导致星形胶质细胞的形态发生改变（图 1）和存活率降低（图 2），提高星形胶质细胞内的氧自由基水平（图 3），同时诱导细胞凋亡（图 4）。然而，所有这些变化都可以被帕瑞昔布逆转。此外，我们发现，Bax、Bcl-2 和 BDNF 的表达水平在 H_2O_2 处理时失调，而在帕瑞昔布预处理时恢复正常。综上所述，帕瑞昔布对 H_2O_2 诱导的氧化应激具有保护作用。

关键词：帕瑞昔布；原代星形胶质细胞；过氧化氢；Bax；Bcl-2；BDNF